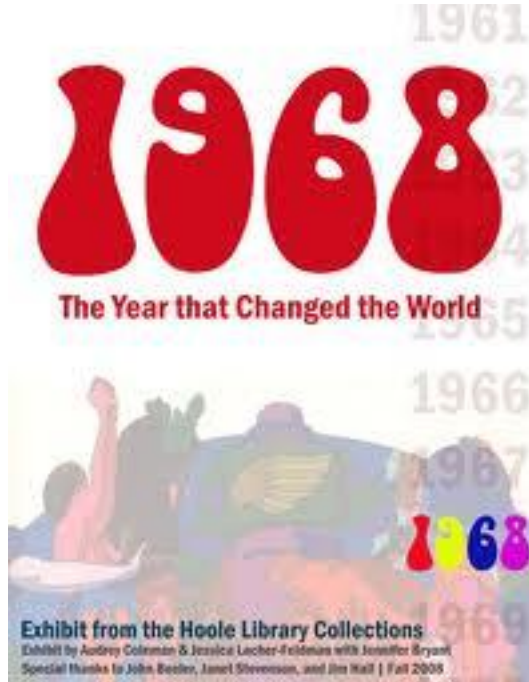


Molecular Genetics of Renal Failure (all genes that cause kidney disease?)



When I was your age, there was polycystic kidney disease, nephronophthisis, Alport syndrome, and an obscure type of congenital nephrotic syndrome in Finland. The idea that we would ever understand how any of these worked, was like landing a man on the moon.



Fred Luft
Charité and Max-Delbrück Center
Berlin, Germany
Luft@charite.de

Focal-segmental glomerulosclerosis (FSGS)

1. Involves 20% of children and 40% of adults with NS
2. Is the most common cause of ESRD in the US
3. Is largely due to “secondary” avoidable causes
4. Is a manifestation of sickle-cell anemia
5. Could be elucidated by the urokinase receptor pathway



[nature.com](#) • [journal home](#) • [archive](#) • [issue](#) • [article](#) • [full text](#)

NATURE MEDICINE | ARTICLE

Circulating urokinase receptor as a cause of focal segmental glomerulosclerosis

Changli Wei, Shafiq El Hindi, Jing Li, Alessia Fornesi, Nelson Goss, Junichiro Sageshima, Dany Margut, S Ananth Karumanchi, Hui-Kun Yap, Moien Saleem, Qingxin Zhang, Benji Hekko, Albert Chaudhuri, Pirouz Daffarlan, Eduardo Salido, Armando Torres, Moro Salifu, Minnie M Sarwal, Franz Schaefer, Christian Morath, Vedat Schwenger, Martin Zeier, Vineet Gupta, David Roth, Maria Pia Ravidelli, et al.

Affiliations | Contributions | Corresponding author

Nature Medicine 17, 952–960 (2011) | doi:10.1038/nm.2411

Received: 05 January 2011 | Accepted: 31 May 2011 | Published online: 31 July 2011

So what about genetics and FSGS???

Focal Segmental Glomerulosclerosis

Vivette D. D'Agati, M.D., Frederick J. Kaskel, M.D., Ph.D., and Ronald J. Falk, M.D.

N Engl J Med 2011; 365:2398-2411 | [December 22, 2011](#)

Type of Disease

Primary (idiopathic) form

Secondary forms

Familial or genetic

Virus-associated

Drug-induced

Adaptive†

Cause

Specific cause unknown; mediated by circulating permeability factors

Mutations in specific podocyte genes*

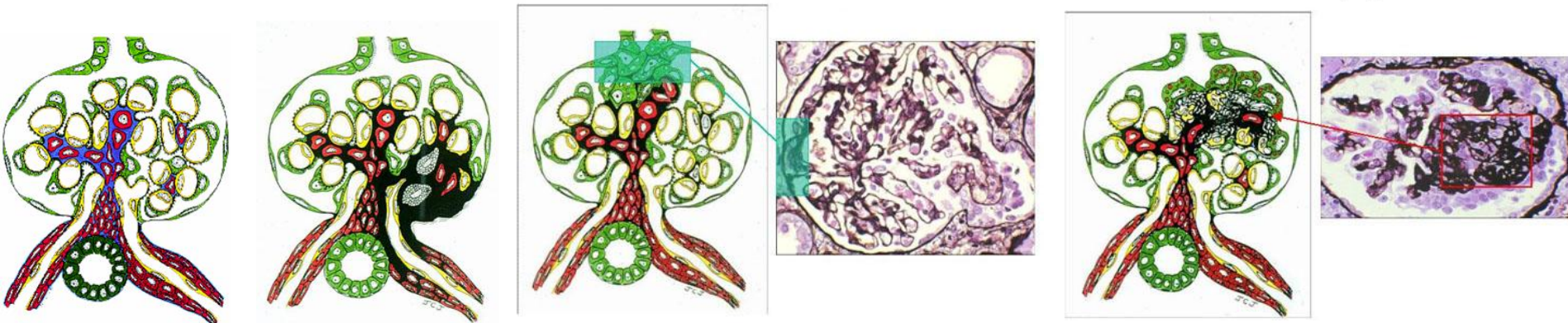
Human immunodeficiency virus type 1, parvovirus B19, simian virus 40, cytomegalovirus, Epstein–Barr virus

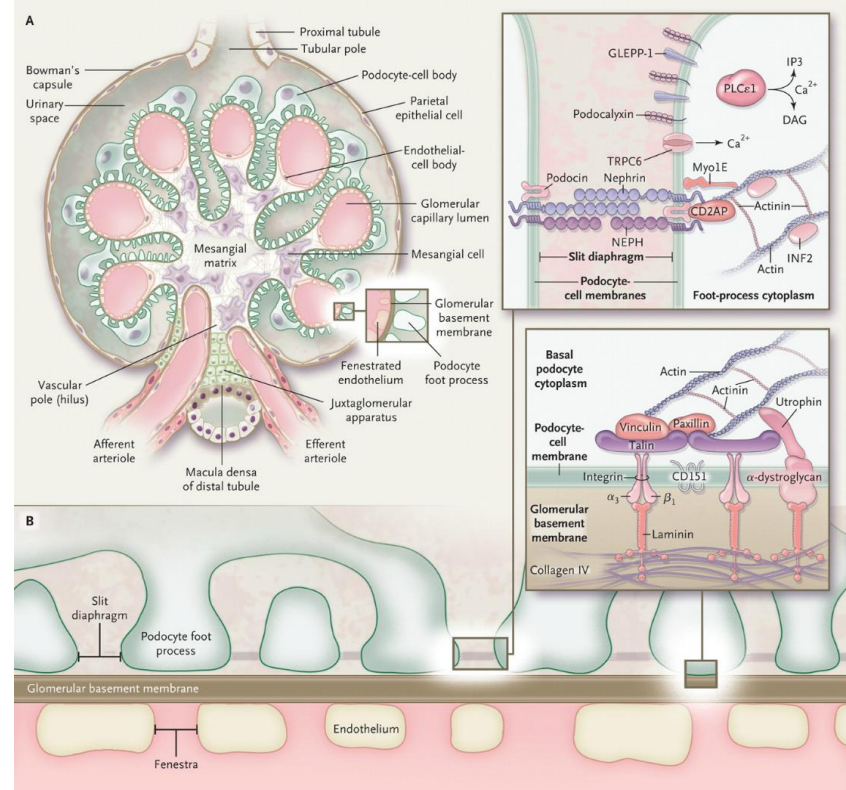
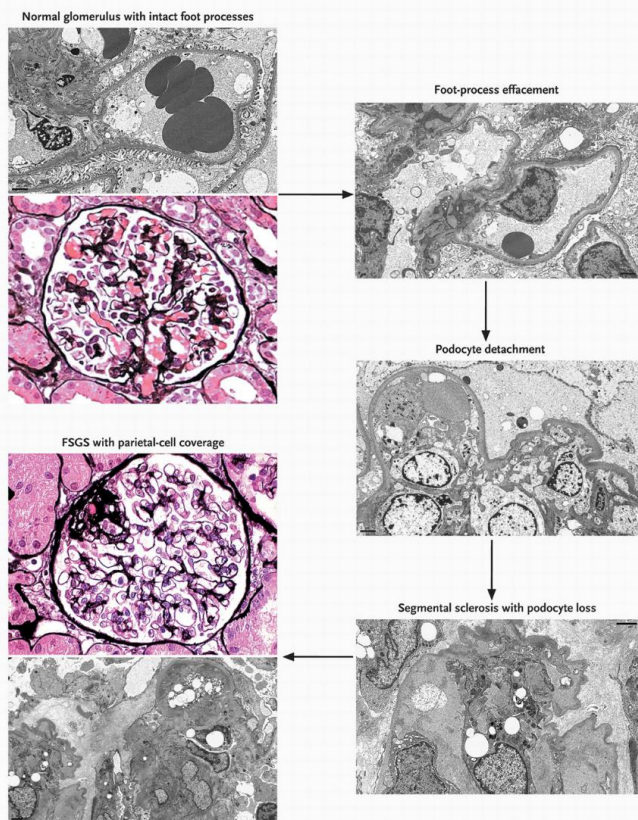
Heroin; interferons alfa, beta, and gamma; lithium; pamidronate; sirolimus; calcineurin-inhibitor nephrotoxicity; anabolic steroids

Conditions with reduced renal mass: oligomeganephronia, very low birth weight, unilateral renal agenesis, renal dysplasia, reflux nephropathy, sequela to cortical necrosis, surgical renal ablation, renal allograft, aging kidney, any advanced renal disease with reduced functioning nephrons

Conditions with initially normal renal mass: systemic hypertension, acute or chronic vaso-occlusive processes (atheroembolization, thrombotic microangiopathy, renal-artery stenosis), elevated body-mass index (obesity, increased lean body mass [e.g., bodybuilding]), cyanotic congenital heart disease, sickle cell anemia

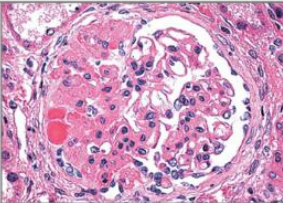
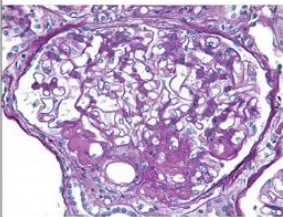
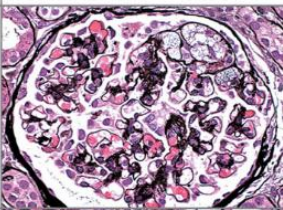
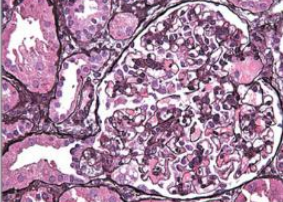
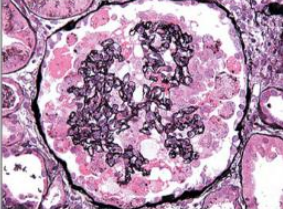
An entire host of these syndromes are genetic; we will discuss three





Nephrin extends into the center of the slit from adjacent podocyte foot processes and form homophilic and heterophilic interactions with **NEPH**. The slit diaphragm complex includes **podocin**. Through interaction with CD2-associated protein (**CD2AP**), the slit diaphragm molecules are linked to the actin cytoskeleton, which is regulated by **α -actinin-4**, inverted formin 2 (**INF2**), and myosin 1E (**Myo1E**). Calcium generated by phospholipase C epsilon 1 (PLC ϵ 1) through diacylglycerol (DAG) and inositol triphosphate (IP3) enters the cell through transient receptor potential cation channel 6 (**TRPC6**) to regulate actin polymerization. At the basal surface, adhesion molecules $\alpha_3\beta_1$ integrin and α -dystroglycan are linked to laminin. Integrin is coupled to the actin cytoskeleton through talin, vinculin, and paxillin, whereas adhesion molecule α -dystroglycan links to actin through utrophin. Negatively charged podocalyxin and glomerular epithelial protein 1 (GLEPP-1) are arrayed on the apical-cell membrane.

Human gene product	Gene	Inheritance	Chromosome
Slit Diaphragm Proteins			
Nephrin	NPHS1	AR	19q13.1
Podocin	NPHS2	AR	1q25-31
CD2-associated protein	CD2AP	AD; rarely AR	6p12
Cell Membrane-Associated Proteins			
Transient receptor potential cation channel 6	TRPC6	AD	11q21-22
Protein tyrosine phosphatase receptor type O (GLEPP1)	PTPRO	AR	12p22
Laminin-β2	LAMB2	AR	3p21
β4-Integrin	ITGB4	AR	17q11
Tetraspanin CD151	CD151	AR	11p15
Cytosolic or Cytoskeletal Proteins			
α-Actinin-4	ACTN4	AD	19q13
Phospholipase C ε1	PLCE1	AR	10q23-24
Myosin heavy chain 9	MYH9	AD	22q12.3
Inverted formin 2	INF2	AD	14q32
Myosin 1E	MYO1E	AR	15q21-26
Nuclear Proteins			
Wilms tumor 1	WT1	AD	11p13
SMARCA-like protein	SMARCA1	AR	2q34-36
Mitochondrial Components			
tRNA ^{Leu}	mtDNA-A3243G	Maternal	mtDNA
Parahydroxybenzoate-polyprenyltransferase	COQ2	AR	4q21-22
Coenzyme Q10 biosynthesis monooxygenase 6	COQ6	AR	14q24.3
Lysosomal Protein			
Lysosomal integral membrane protein (LIMP) type 2	SCARB2	AR	4q13-21
Unknown Cellular Location			
Apolipoprotein L1	APOL1	AR	22q12

Histologic Subtype	Glomerular Lesion
NOS	
Perihilar	
Cellular	
Tip	
Collapse	

Generic FSGS
Genetic forms

Obesity,
hypertension

Primary or
secondary

Best prognosis

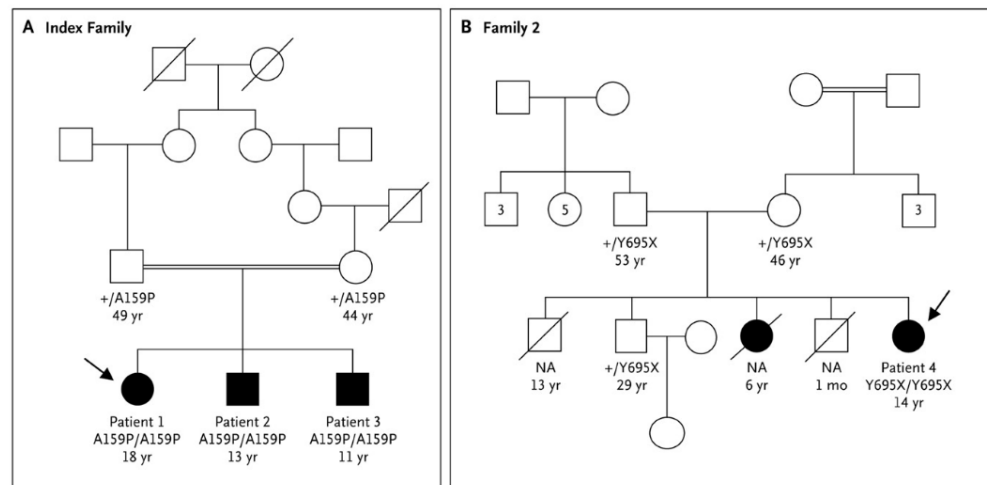
HIV, parvovirus
SV40, EBV, CMV,
pamidronate,
interferon, CNI, CAN

MYO1E Mutations and Childhood Familial Focal Segmental Glomerulosclerosis

Caterina Mele, Biol.Sci.D., Paraskevas Iatropoulos, M.D., Roberta Donadelli, Biol.Sci.D., Andrea Calabria, Eng.D., Ramona Maranta, Biol.Sci.D., Paola Cassis, Ph.D., Simona Buelli, Ph.D., Susanna Tomasoni, Ph.D., Rossella Piras, Chem.Pharm.D., Mira Krendel, Ph.D., Serena Bettoni, Biotech.D., Marina Morigi, Ph.D., Massimo Delledonne, Ph.D., Carmine Pecoraro, M.D., Isabella Abbate, Ph.D., Maria Rosaria Capobianchi, Ph.D., Friedhelm Hildebrandt, M.D., Edgar Otto, M.D., Franz Schaefer, M.D., Fabio Macchiardi, M.D., Fatih Ozaltin, M.D., Sevinc Emre, M.D., Tulin Ibsirlioglu, Ph.D., Ariela Benigni, Ph.D., Giuseppe Remuzzi, M.D., and Marina Noris, Ph.D. for the PodoNet Consortium

We performed whole-genome linkage analysis followed by high-throughput sequencing of the positive-linkage area in a family with autosomal recessive focal segmental glomerulosclerosis (index family) and sequenced a newly discovered gene in 52 unrelated patients with focal segmental glomerulosclerosis. Immunohistochemical studies were performed on human kidney-biopsy specimens and cultured podocytes. Expression studies in vitro were performed to characterize the functional consequences of the mutations identified.

Ala-
Pro-



A non-muscle myosin

Whole-genome linkage analysis was performed in the index family with the use of an array of 1 million single-nucleotide polymorphisms (SNPs).

Tyr-
Stop-

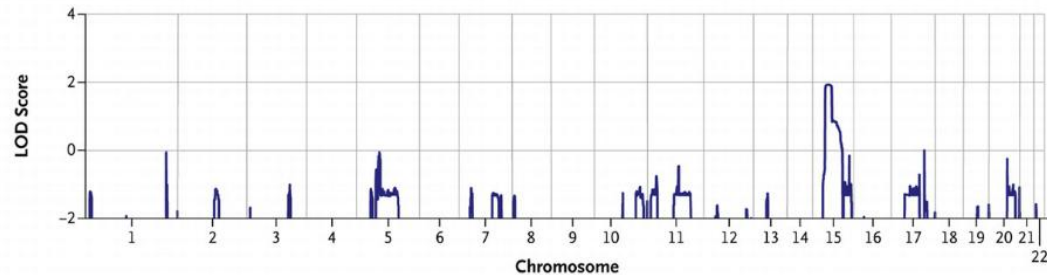
The family tree shows

1. Incest
2. Autosomal dominant
3. Autosomal recessive
4. Spontaneous mutations
5. Cannot be determined

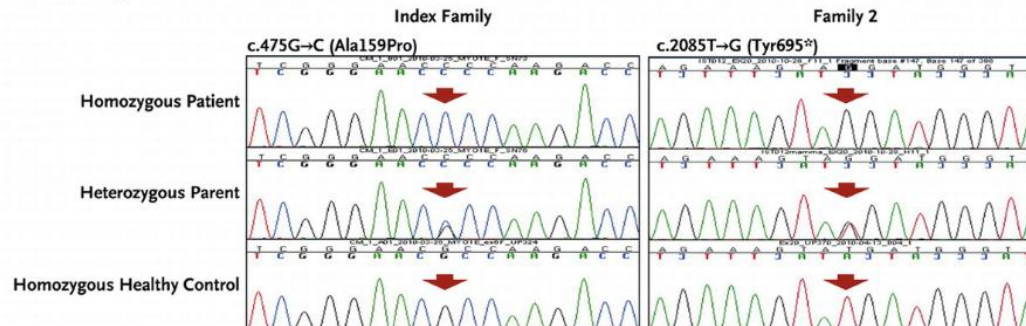
Patient No.	Age at Diagnosis	Age at Onset of ESRD	Treatment	Finding on Renal Biopsy	First Observation			Last Observation			
	Age	Urinary Protein			Serum Creatinine	Age	Urinary Protein	Serum Creatinine			
		yr			yr	g/24 hr	mg/dl	yr	g/24 hr	mg/dl	
Index family											
Patient 1	9	13	Glucocorticoids (NR), cyclosporine (NR), ACE inhibitor (NR)	Advanced FSGS	9	3.00	0.6	18	0.05†	1.1†	
Patient 2	4	—	Cyclosporine (PR), ACE inhibitor (PR)	FSGS	4	1.56	0.4	13	0.53	0.7	
Patient 3	2	—	Glucocorticoids (NR), cyclosporine (PR), ACE inhibitor (PR)	FSGS	2	3.40	0.4	11	0.59	0.7	
Family 2											
Patient 4	1	—	Glucocorticoids (NR), cyclosporine (PR), ACE inhibitor (PR)	FSGS	1	+++‡	0.3	14.5	2.8	0.3	

900 K SNP chip
for linkage

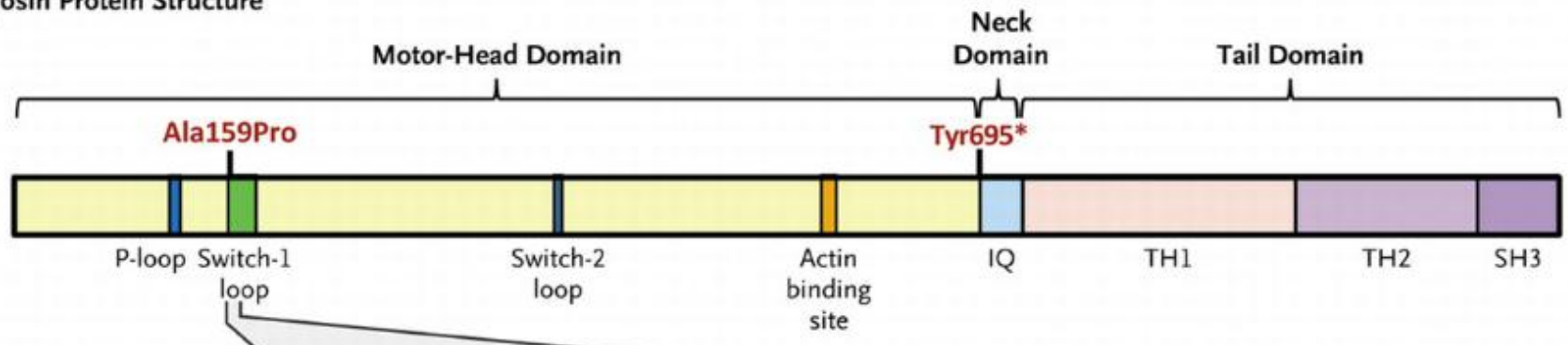
A Whole-Genome Multipoint Linkage Analysis in Index Family



B Direct Sequencing

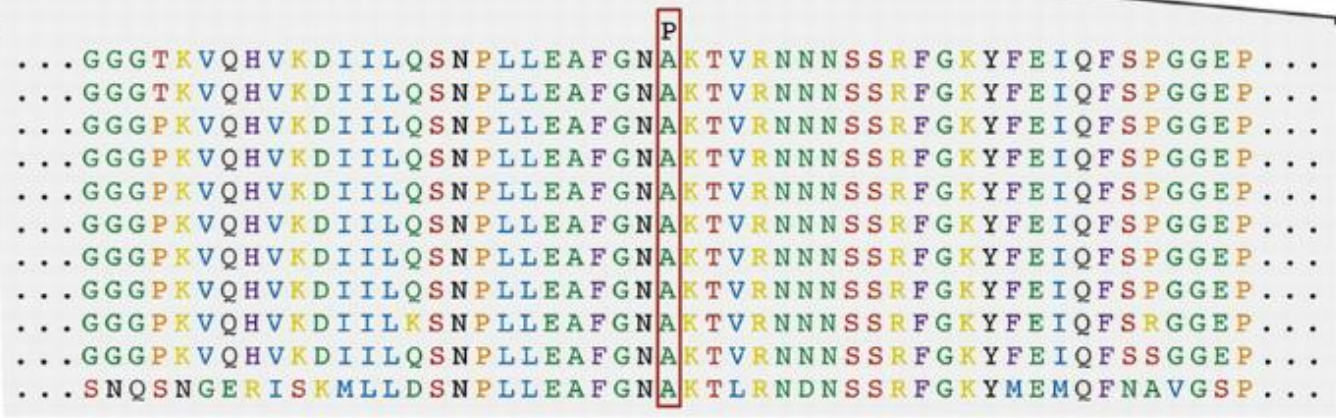


C Myosin Protein Structure

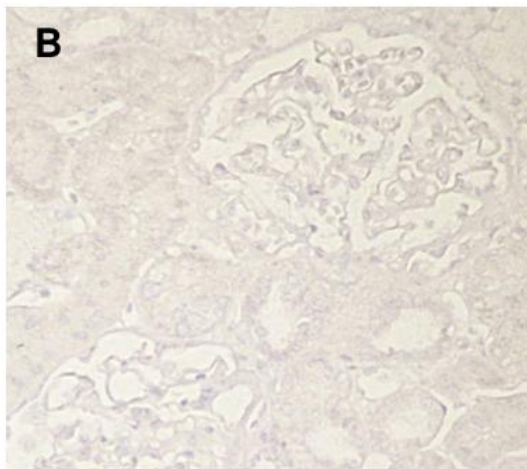
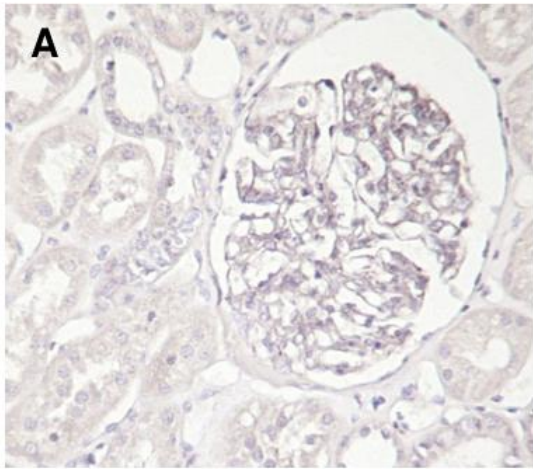


D Sequence Alignment of Myo1E and Homologues

- Mutation
- Homo sapiens*
 - Pan troglodytes*
 - Macaca mulatta*
 - Mus musculus*
 - Rattus norvegicus*
 - Canis familiaris*
 - Equus caballus*
 - Gallus gallus*
 - Xenopus laevis*
 - Danio rerio*
 - Dictyostelium discoideum*

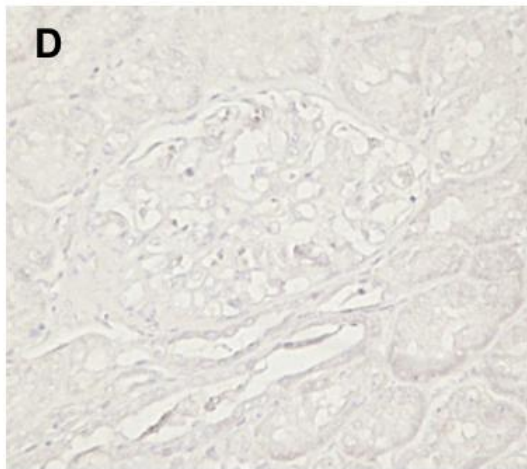
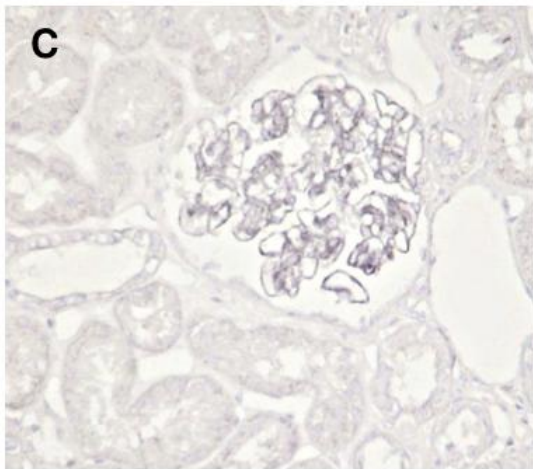


Whole-genome linkage analysis was performed in the index family with the use of an array of 1 million single-nucleotide polymorphisms (SNPs).

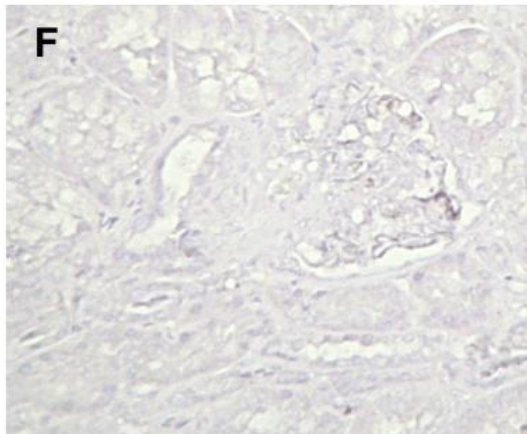
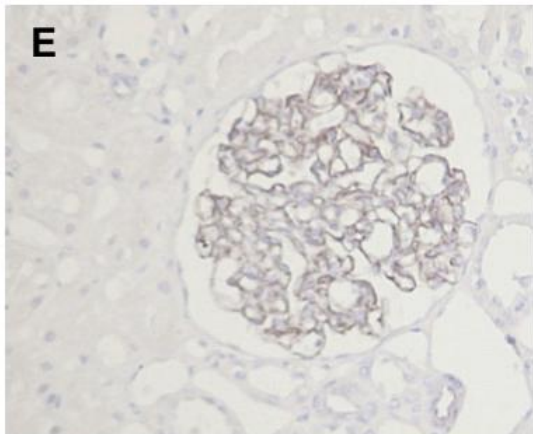
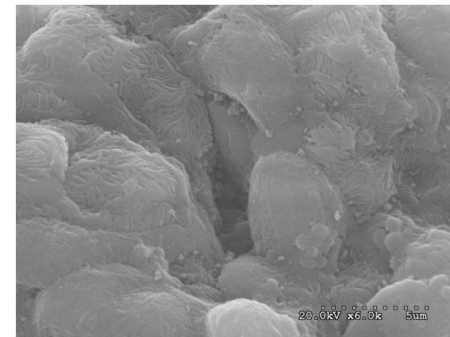


Immunoperoxidase staining of Myo1E, synaptopodin and podocin in control human and patient 4 biopsies.

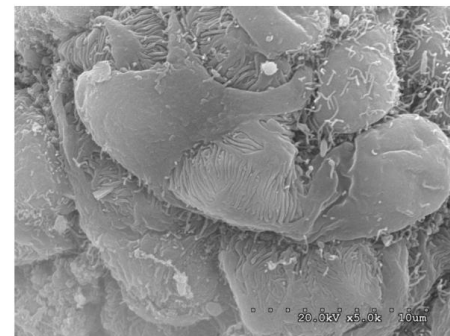
Scanning electron microscopy images of wild-type and myo1e-ko mouse glomeruli showing podocyte microvillous transformation.

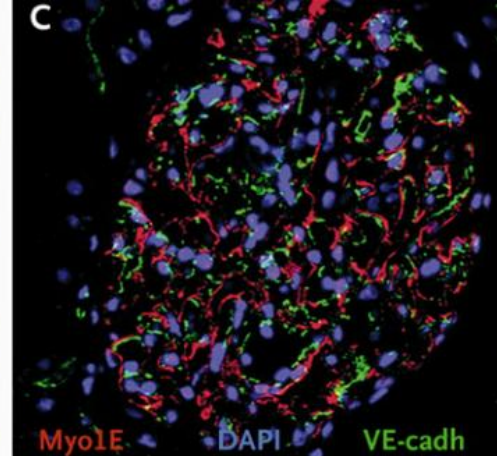
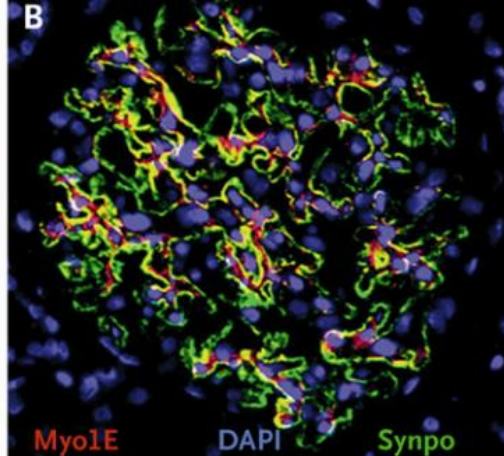
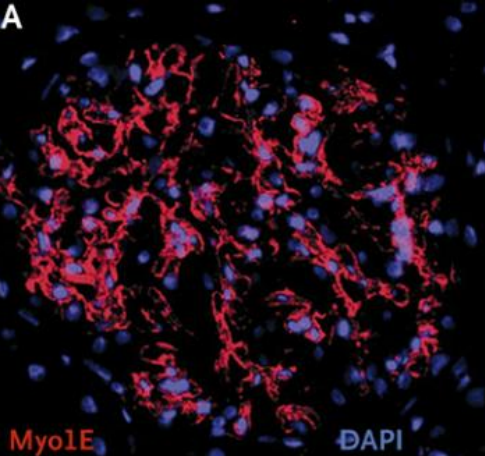


WT

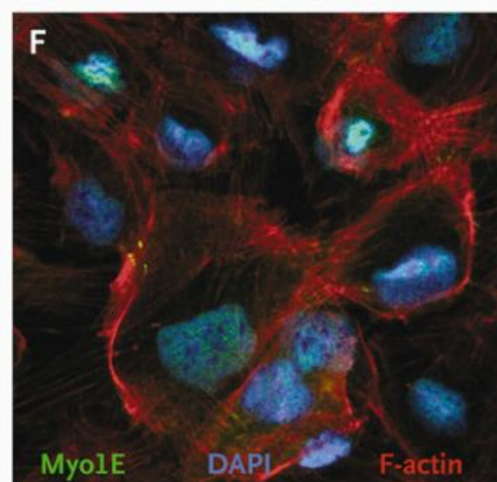
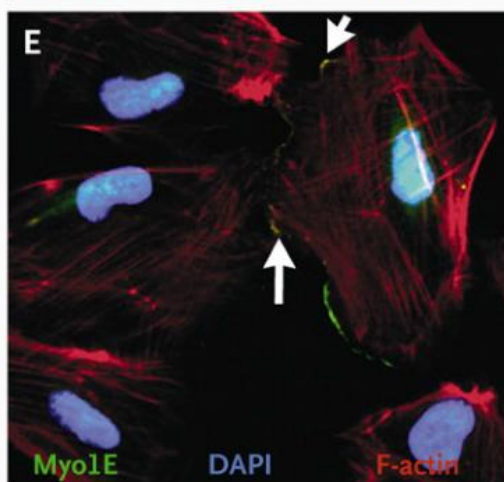
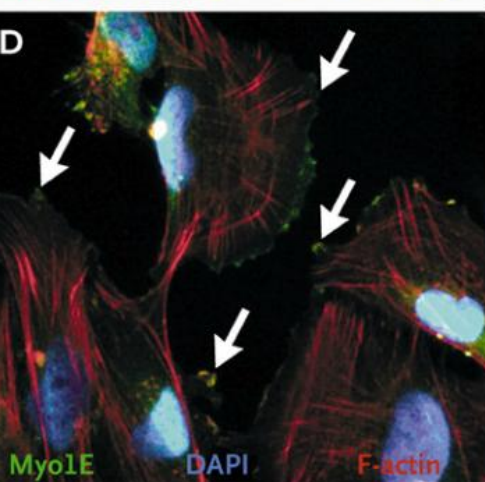


KO

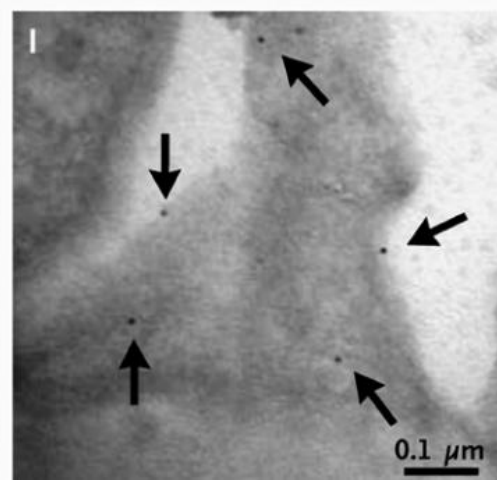
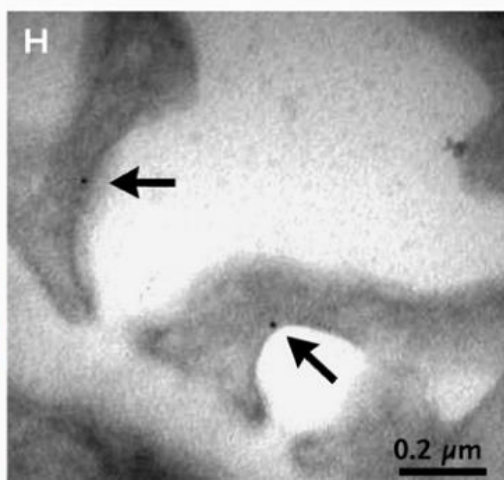
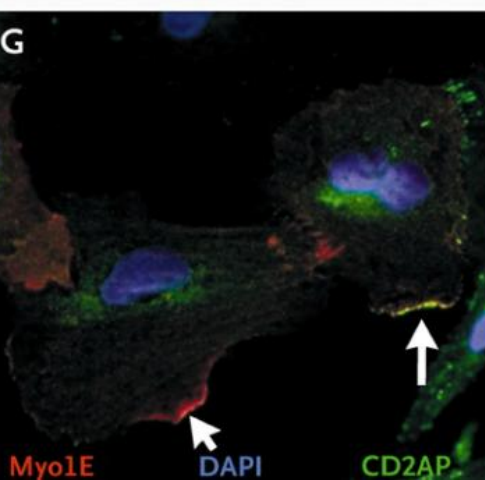




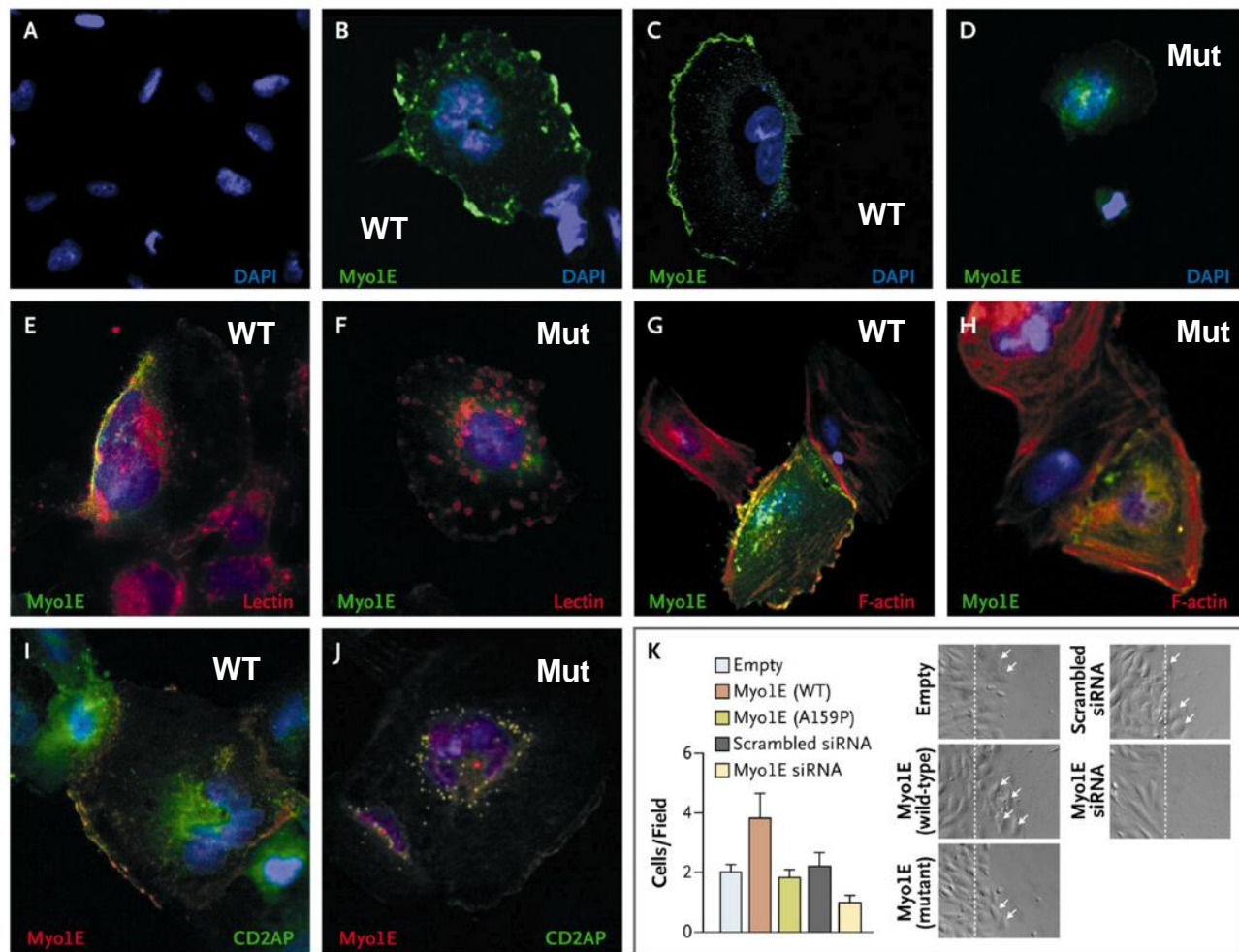
A,B,C are normal kidney. Myo1E (red) is mainly expressed in podocytes (synpo green), as is the case in mice.



D, E, F, are cultured human podocytes. Myo1E (red) localized close to the cytoplasmic membrane, with enrichment at the lamellipodia tips.

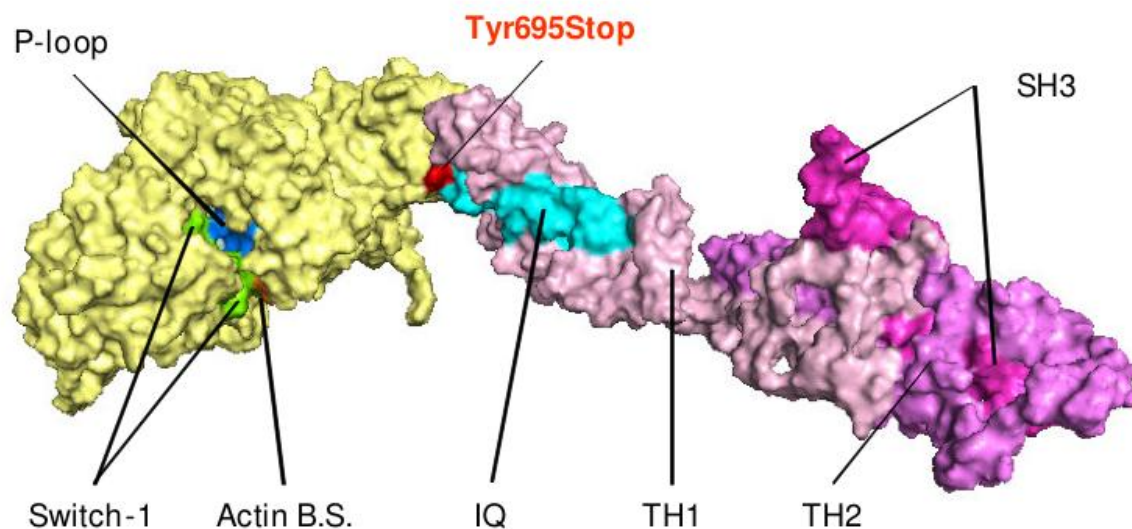
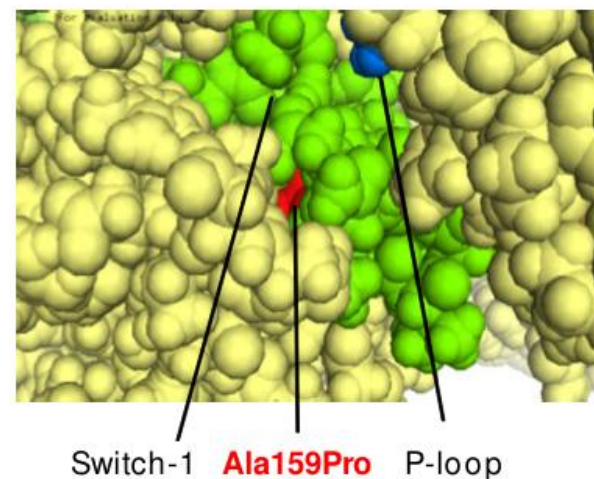


H, I, are immuno-gold labeling for Myo1E in control human glomeruli revealed gold particles almost exclusively on the cytoplasmic side of the podocyte plasma membrane



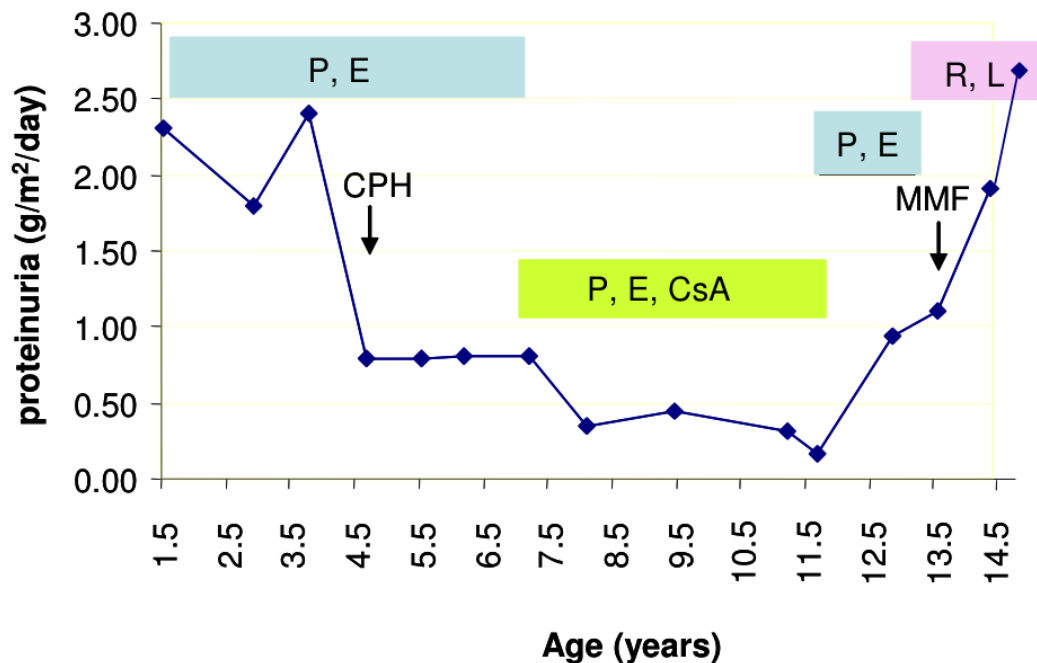
Human podocytes transfected with green fluorescent protein (GFP)–tagged wild-type Myo1E or E753K, I531M, D465N, and F307L (control SNPs) showed predominant localization at the plasma membrane, whereas podocytes transfected with GFP-tagged mutant A159P Myo1E showed diffuse cytoplasmic localization, which at a higher plasmid dose acquired a punctate pattern

Wild-type Myo1E overexpression increased human podocyte motility (Figure 4K). In contrast, A159P Myo1E had no effect on podocyte motility. Conversely, Myo1E knockdown in human podocytes (Panel K) and Myo1E knockout in mouse podocytes impaired migration (unpublished data).

A**B**

Panel A shows views of the Myo1E protein showing the ATP pocket with the Switch-1 (green) and the P-loop (blue) domains, the actin binding site (orange), the IQ (light blue), the TH1 (pink), the TH2 (violet) and the SH3 (dark violet) domains. A detail of the ATP pocket with the position of the Ala159 is shown in panel B (red).

Nonmuscle myosin activity generates tension, and the interaction among actin, myosins, and **alpha-actinin-4** probably allows the foot processes to generate the contractile forces that help the glomerular capillaries to resist the high intraluminal hydrostatic pressure and to change their morphologic structure actively, modifying the permeability of the glomerular filtration barrier. **MYO1E** mutations have a role in focal segmental glomerulosclerosis and suggest the importance of Myo1E in podocyte homeostasis and the consequent integrity of the glomerular filtration barrier.



Nature Medicine **14**, 931 - 938 (2008)

Published online: 24 August 2008 | doi:10.1038/nm.1857

The actin cytoskeleton of kidney podocytes is a direct target of the antiproteinuric effect of cyclosporine A

Christian Faul^{1,2}, Mary Donnelly^{1,2}, Sandra Merscher-Gomez^{1,2}, Yoon Hee Chang^{2,5}, Stefan Franz^{2,5}, Jacqueline Delfgaauw^{2,5}, Jer-Ming Chang³, Hoon Young Choi², Kirk N Campbell^{1,2}, Kwanghee Kim², Jochen Reiser^{1,4} & Peter Mundel^{1,2}

Beneficial effect of CsA on proteinuria is not dependent on NFAT inhibition in T cells, but rather results from the stabilization of the actin cytoskeleton in kidney podocytes.

This patient has

1. Lead poisoning
2. Peroneal palsy
3. Flat feet
4. Proteinuria



Charcot-Marie-Tooth disease is the most common inherited disorder of the peripheral nervous system. The disease is characterized by a progressive muscle weakness and atrophy, sensory loss, foot (and hand) deformities and steppage gait. While many of the genes associated with axonal CMT have been identified, to date it is unknown which mechanism(s) causes the disease. However, genetic findings indicate that the underlying mechanisms mainly converge to the axonal cytoskeleton.

INF2 Mutations in Charcot–Marie–Tooth Disease with Glomerulopathy

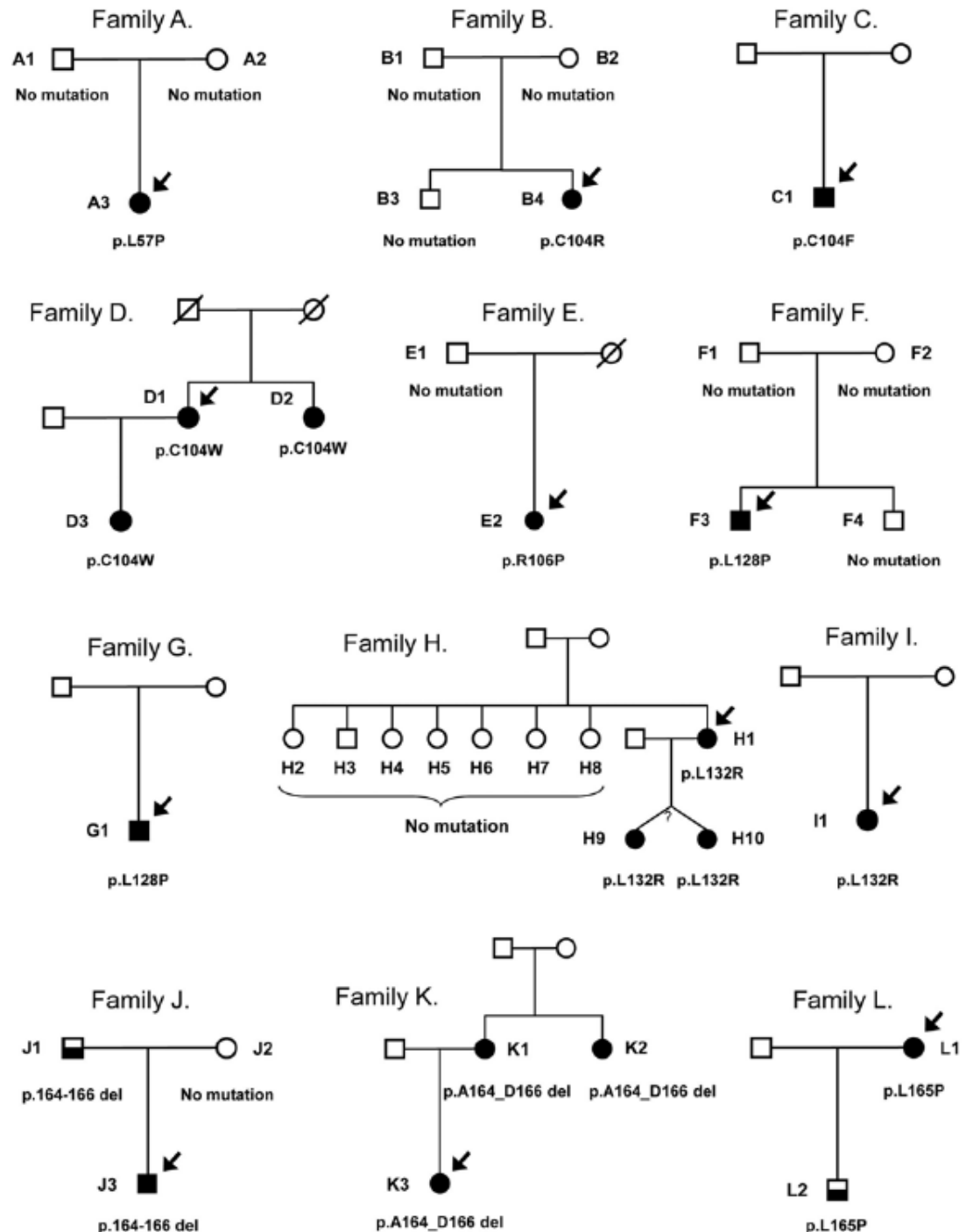
Olivia Boyer, M.D., Ph.D., Fabien Nevo, M.Sc., Emmanuelle Plaisier, M.D., Ph.D.,
Benoit Funalot, M.D., Ph.D., Olivier Gribouval, M.Sc., Geneviève Benoit, M.D.,
Evelyne Huynh Cong, M.Sc., Christelle Arrondel, M.Sc., Marie-Josèphe Tête, M.D.,
Rodrick Montjean, Ph.D., Laurence Richard, M.Sc., Alexandre Karras, M.D.,
Claire Pouteil-Noble, M.D., Ph.D., Leila Balafrej, M.D., Alain Bonnardeaux, M.D., Ph.D.,
Guillaume Canaud, M.D., Christophe Charasse, M.D., Jacques Dantal, M.D., Ph.D.,
Georges Deschenes, M.D., Ph.D., Patrice Deteix, M.D., Odile Dubourg, M.D., Ph.D.,
Philippe Petiot, M.D., Dominique Pouthier, M.D., Eric Leguern, M.D., Ph.D.,
Anne Guiochon-Mantel, M.D., Ph.D., Isabelle Broutin, Ph.D.,
Marie-Claire Gubler, M.D., Sophie Saunier, Ph.D., Pierre Ronco, M.D., Ph.D.,
Jean-Michel Vallat, M.D., Miguel Angel Alonso, Ph.D.,
Corinne Antignac, M.D., Ph.D., and Géraldine Mollet, Ph.D.

inverted formin 2

Mutations in inverted-formin 2 (INF2) were recently identified in patients with autosomal dominant FSGS. INF2 encodes a formin protein that interacts with the Rho-GTPase CDC42 and myelin and lymphocyte protein (MAL) that are implicated in essential steps of myelination and myelin maintenance. We therefore hypothesized that INF2 may be responsible for cases of Charcot-Marie-Tooth neuropathy associated with FSGS. We performed direct genotyping of INF2 in 16 index patients with Charcot-Marie-Tooth neuropathy and FSGS who did not have a mutation in PMP22 or MPZ, encoding peripheral myelin protein 22 and myelin protein zero, respectively. Histologic and functional studies were also conducted.

Mode of inheritance

1. X-linked recessive
2. X-linked dominant
3. Autosomal recessive
4. Autosomal dominant
5. Damned if I know!



Mutations in
PMP22 or MPZ
were ruled out in all
patients.

		Armadillo repeat 1				
		α		α		
		αααααα		αααααααααααααααα		ααα
Human INF2	-----	-----ELCIRLLQMPSSVVNYSGLRKRLEGGSGGWM				65
Mouse INF2	-----	-----ELCIRLLQMPSSVVNYSGLRKRLESSGGGWM				65
Opposum INF2	-----	-----ELCIRLLQMPSSVVNYSGLRKRLESSGGGWL				65
Xenopus INF2	-----	-----ELCIRLLQIPSSVVNYSGLRKRLESSGGGWM				65
Human DIAPH1	KREMVSQYLTSKAGMSQKESSKASMMYIQELRSLGRDMLPLSCLESLSRVN					180
Mouse mDial	KREMVSQYLHTSKAGMNQKESSRSAMMYIQELRSLGRDMLHLLSCLESLSRVN					171
		P		P		
		Armadillo repeat 2				
		α		α		
		αα		αααααααααααααααα		αααααα
Human INF2	VQFLEQSGLDLLEALARLSGR--GVARISDALLQCTVCSVRVAMNSRQGTIEYILSNQG					123
Mouse INF2	VQFLEQSGLDLLEALARLSGR--GVARISDALLQCTCISVRVAMNSRQGTIEYILSNQG					123
Opposum INF2	VQFLEQSGLDLLEALARLSGR--GVARIADALLQCTCISVRVAMNSRQGTIEYILSNQG					123
Xenopus INF2	VQFLEQSGLDLLEALDRLSGR--GVARIADALLQCTICVTRTLNMSHRGTIEYIVNNEG					123
Human DIAPH1	QTGF-AEGLASLDLTKRLHDEKEETSGYDSRNKHEIIRCLKAFMNNKFGIKTMLEETE					239
Mouse mDial	QTGF-AEGLASLDLTKRLHDEKEETSGYDSRNQHEIIRCLKAFMNNKFGIKTMLEETE					230
		P		R P F		
		Armadillo repeat 3				
		α		α		
		ααααααα		αααααααααααααααα		ααα
Human INF2	YVRQLSQALDTSNMVKKQVFELLAALCIYS-PEGHVLTLDALDHYKTVCSQQYRFSIVM					182
Mouse INF2	YVRQLSQALDTSNMVKKQVFELLAALCIYS-PEGHVLTLDALDHYKTVCSQQYRFSIVM					182
Opposum INF2	YVCKLSEALDTSNMVKKQVFELLAALCIYS-PEGHQTLDALDHYKTVKVSQQYRFSIVM					182
Xenopus INF2	YVRQLSQALDTSNMVKKQVFELLAALCIYS-PEGHALSLEALDHYKAVKVSQQYRFSIVM					182
Human DIAPH1	GILLVRAMPDPAVNMMDIAAKLLSALCILPQPEDMNERYLEAMTERAMDEVEERFPQLL					299
Mouse mDial	GILLVRAMPDPAVNMMDIAAKLLSALCILPQPEDMNERYLEAMTERAMDEVEERFPQLL					290
		P		P del		H
		Armadillo repeat 4				
		α		α		
		ααα		αααααααααααααααα		ααα
Human INF2	NELSGSDNVPPVVTLLSVNAVILGPEDLRAARTQLRNEFFIGQLDLRLARLDLEDADLL					242
Mouse INF2	SELSDSDNVPPVVTLLSVNAVILGPEDLRAARTQLRNEFFIGQLDLRLARLDLEDADLL					242
Opposum INF2	NELSSTDNVPPVVTLLSVNAVILGTEELRAARTQLRNEFFIGQLDLRLTKRDLTDLDLL					242
Xenopus INF2	NELSTSDNVPPVVTLLSAINAIIFGTEELRKRQVLRNEFFIGQLDLRLTKRDLTDLDLL					242
Human DIAPH1	DGLKSGTTIALKVGCQLQINALITPAEELDFRVHRSLEMLRGLHQVLDLREIENEDMR					359
Mouse mDial	DGLKSGTSIALKVGCLQINALITPAEELDFRVHRSLEMLRGLHQVLDLREIENEDMR					350
		K	P	H	R	C
						Q
						W

B

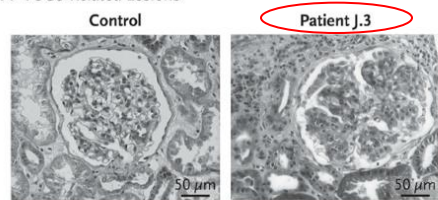


INF2 mutations account for 12 to 17% of autosomal dominant cases of FSGS. The gene encodes a member of the diaphanous-related formin family, which is involved in remodeling the actin and microtubule cytoskeletons. INF2 possesses functional domains characteristic of other diaphanous-related formins: an N-terminal diaphanous-inhibitory domain (DID), the formin homology domains FH1 and FH2, and a C-terminal diaphanous-autoregulatory domain (DAD). However, INF2 has a unique ability to promote not only actin polymerization but also filament severing and depolymerization.

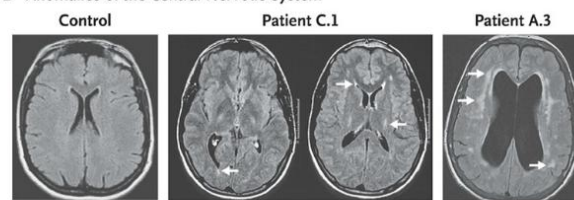
All were new mutations located in exons 2 and 3, which encode the DID domain (Panel A). All caused nonconservative changes in highly conserved amino acids. we mapped mutants associated with FSGS alone and those associated with FSGS and Charcot–Marie–Tooth neuropathy onto a human INF2 DID in silico model (Panel B).

All involved DID residues, mutations in the two groups of patients were distinctly localized, the latter being located mostly in the second and third DID armadillo repeats and the former mostly in the fourth armadillo repeat

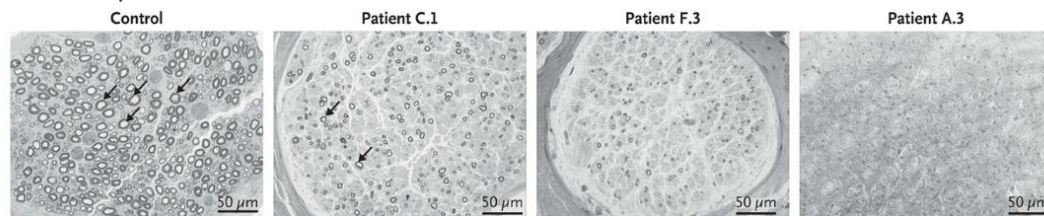
A FSGS-Related Lesions



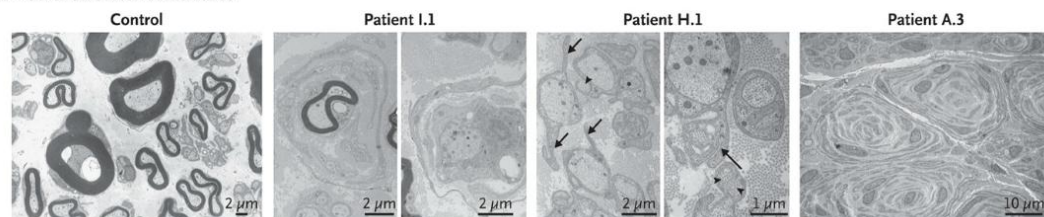
B Anomalies of the Central Nervous System



C Decreased Myelinated Fibers in Sural Nerves



D Other Sural-Nerve Anomalies

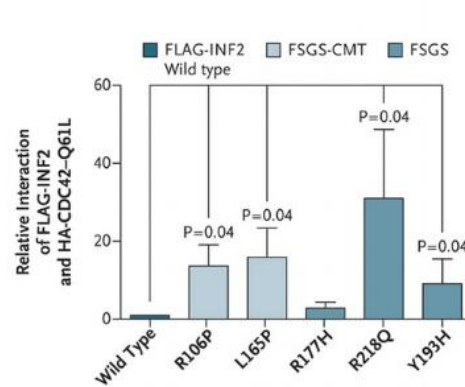
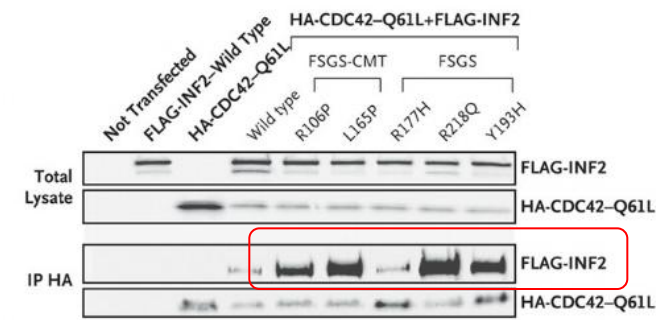


All patients had FSGS, but full-blown nephrotic syndrome was noted in only 5. Magnetic resonance imaging of the brain showed central nervous system anomalies characterized by white-matter hyperintensity and ventricular dilation, which were more severe in the older patient. Sural-nerve biopsy specimens all showed a pattern of lesions with a combination of axonal and demyelinating changes, characterized by a **marked decrease in myelinated fibers**, as compared with that in age-matched controls, and numerous multilayered “onion bulbs”. These data suggest an intermediate Charcot–Marie–Tooth phenotype in patients with *INF2* mutations.

Sensorineural
Hearing LossBrain MRI
AnomalyNerve Conduction
VelocityESP Nerve Median Nerve
m/sec

Yes	Yes	No potential	No potential
No	ND	No potential	No potential
No	Yes	No potential	No potential
No	ND	<30	<30
Yes	ND	No potential	32
No	ND	No potential	23
Yes	ND	No potential	No potential
No	ND	No potential	42
No	ND	No potential	30–32
Yes	ND	ND (patient declined)	
No	ND	15–28	45
No	ND	No potential	41–42

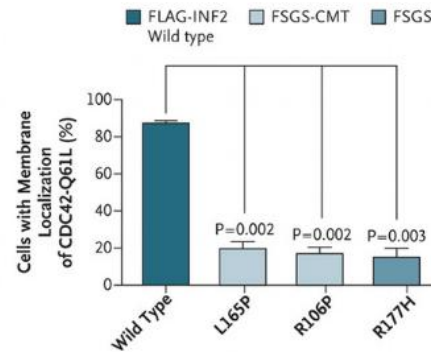
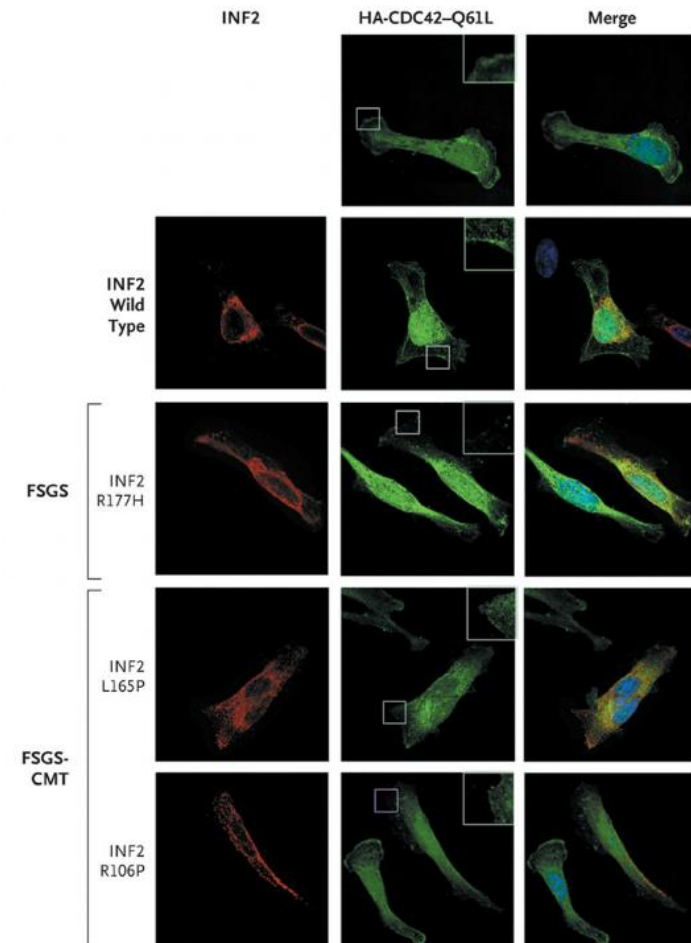
A



Enhanced interaction

CDC42 is an actin-regulation Rho-GTPase

B



Failed membrane placement

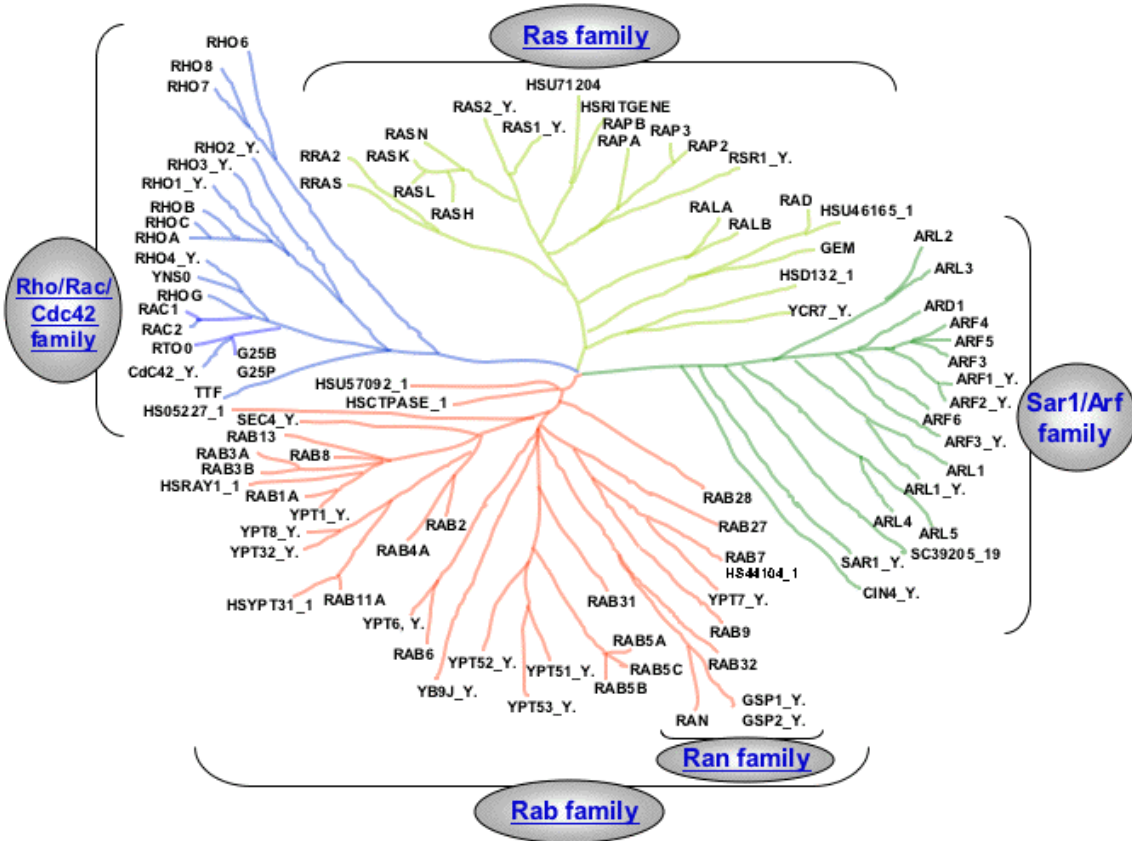
We investigated whether the mutations in INF2 proteins affect their binding to CDC42, an actin-regulating Rho-GTPase known to interact with the INF2 DID. An enhanced interaction was observed between the INF2 mutants and a constitutively active form of CDC42 (CDC42-Q61L) as compared with the wild-type INF2 protein (panel A and B). INF2 mutants affected the subcellular localization of CDC42-Q61L, with the fraction of active CDC42 at the plasma membrane being lost in a large proportion of mutant cells as compared with cells expressing wild-type INF2 (panel C).

The formin INF2 as a crucial molecular entity in the occurrence of FSGS and Charcot-Marie-Tooth neuropathy provides additional insight into the role of similar cellular machinery in podocytes and Schwann cells, even though these two highly specialized cell types have distinct functions.

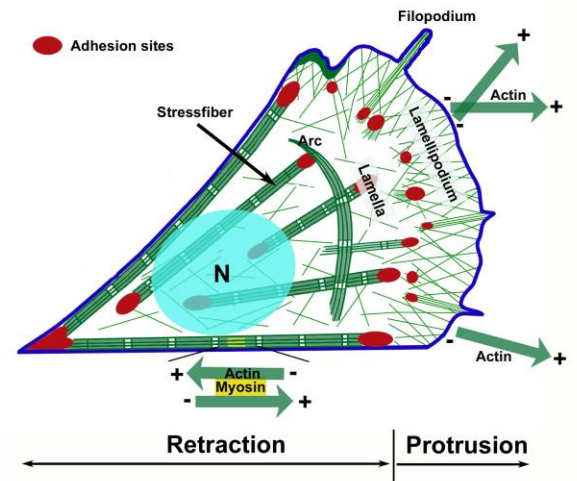
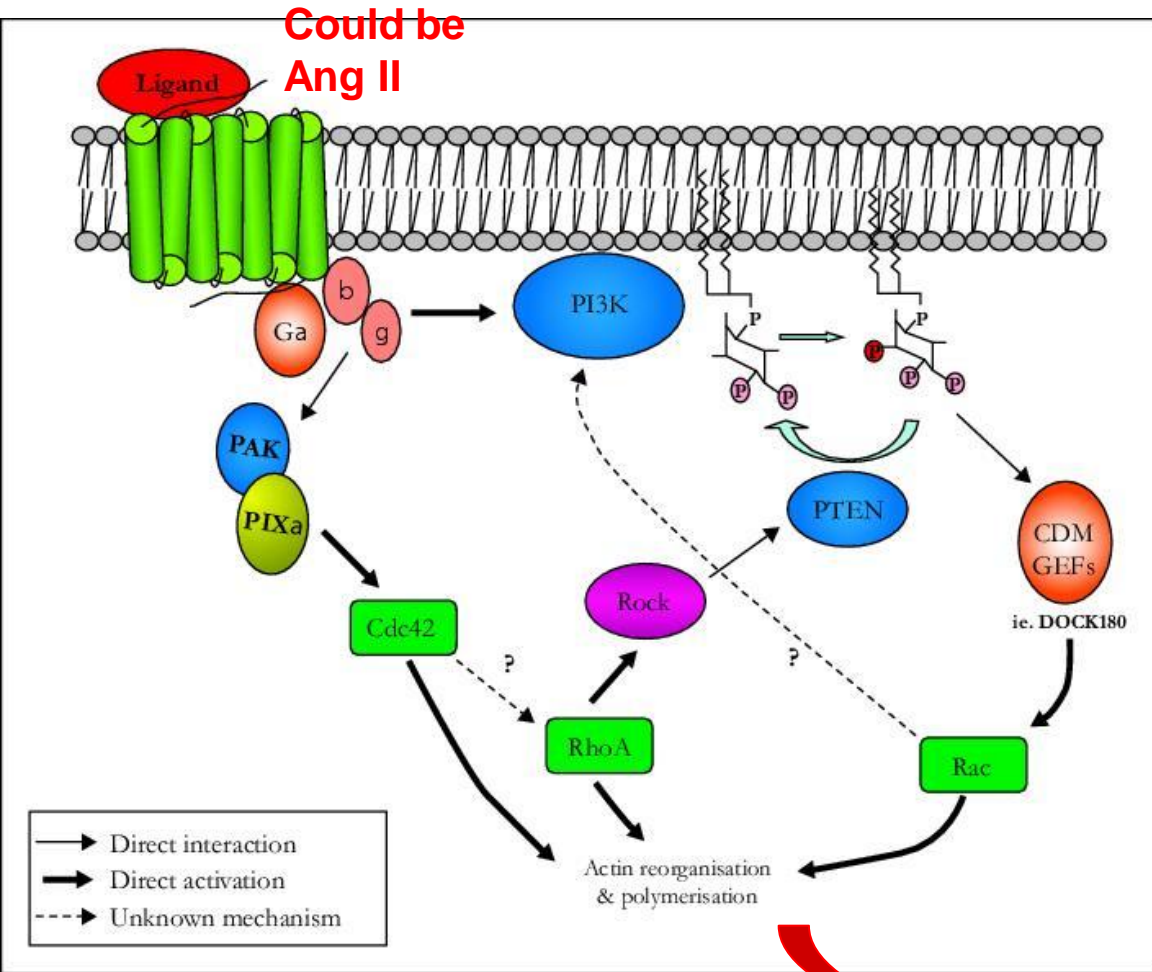
Stressed-out podocytes seeking to avoid proteinuria

1. Rearrange their actin cytoskeleton
2. Retract or efface their foot processes
3. Abandon their RhoA-dependent stationary state
4. Assume a CDC42- and Rac1-dependent migratory state
5. Require a functioning Rac1 GTPase-activating (GAP) protein

**Like for instance
Arhgap24**



Ras homolog gene family, member A (RhoA) is a small GTPase protein known to regulate the actin cytoskeleton in the formation of stress fibers. In humans, it is encoded by the gene RHOA. It acts upon two known effector proteins: ROCK1 (Rho-associated, coiled-coil containing protein kinase 1) and DIAPH1 (diaphanous homolog 1 (Drosophila)). RhoA is part of a larger family of related proteins known as the Ras superfamily; proteins involved in the regulation and timing of cell division.

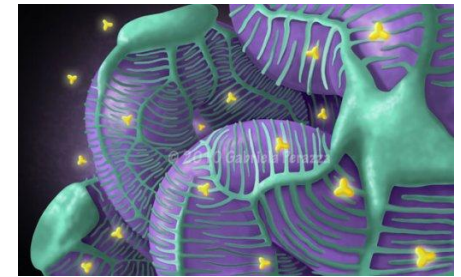


Effacement

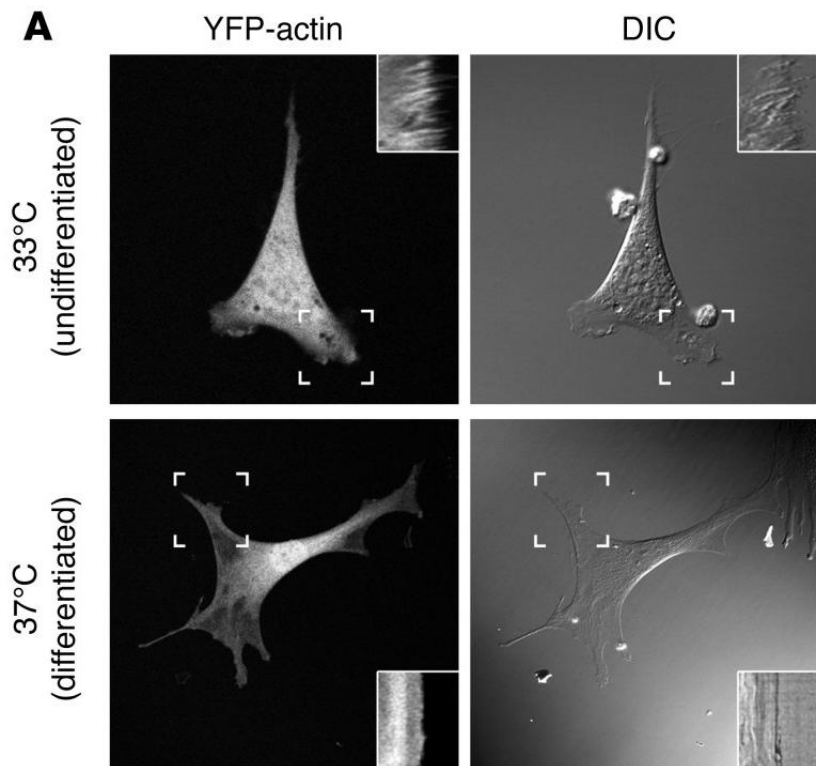
Stationary

Arhgap24 inactivates Rac1 in mouse podocytes, and a mutant form is associated with familial focal segmental glomerulosclerosis

Shreeram Akilesh¹, Hani Suleiman², Haiyang Yu², M. Christine Stander², Peter Lavin³, Rasheed Gbadegesin⁴, Corinne Antignac⁵, Martin Pollak⁶, Jeffrey B. Kopp⁷, Michelle P. Winn³ and Andrey S. Shaw²



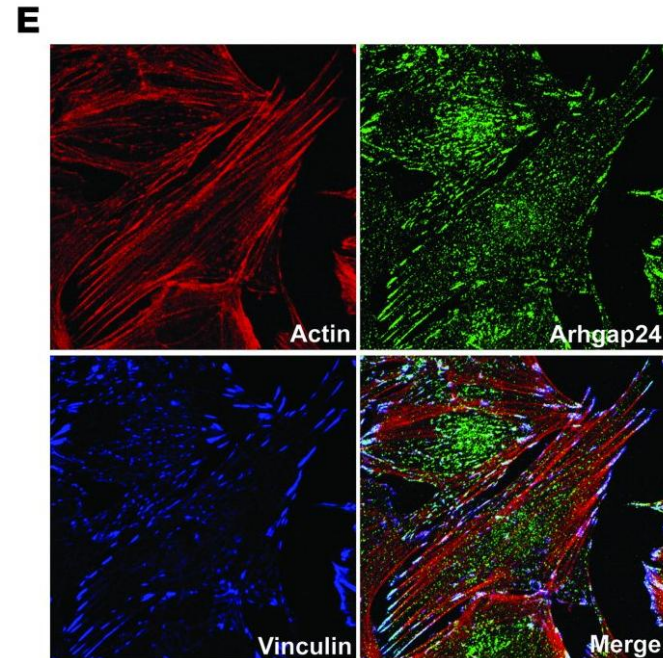
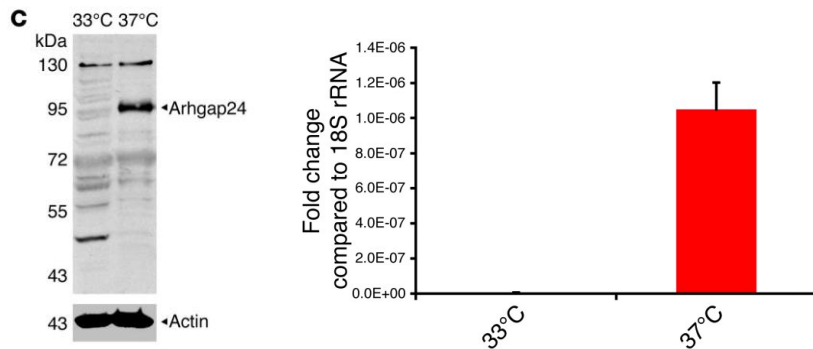
We found that decreased membrane ruffling in differentiated podocytes was dependent on the presence of the **GTPase-activating protein (GAP), Rho-GAP 24 (Arhgap24)**. Previous work from Stossel and colleagues has shown that Arhgap24 (also known as Filamin A-binding RhoGAP [FilGAP]) is a GAP for Rac1 and that it suppresses lamellipodia formation and cell spreading downstream of RhoA signaling. Their work showed that the highest level of Arhgap24 transcript was present in the kidney. Here we show that Arhgap24 was highly expressed in podocytes of the kidney and was upregulated as these cells differentiate in vivo. **The ARHGAP24 gene is highly conserved, implying an important role for the gene product.** When we sequenced the DNA from patients with FSGS, we identified a loss-of-function mutation in the ARHGAP24 gene in a kindred with familial kidney disease. Taken together, these results suggest that Arhgap24 controls the RhoA-Rac1 signaling balance in podocytes that appear to be dysregulated in proteinuric kidney diseases, such as FSGS.



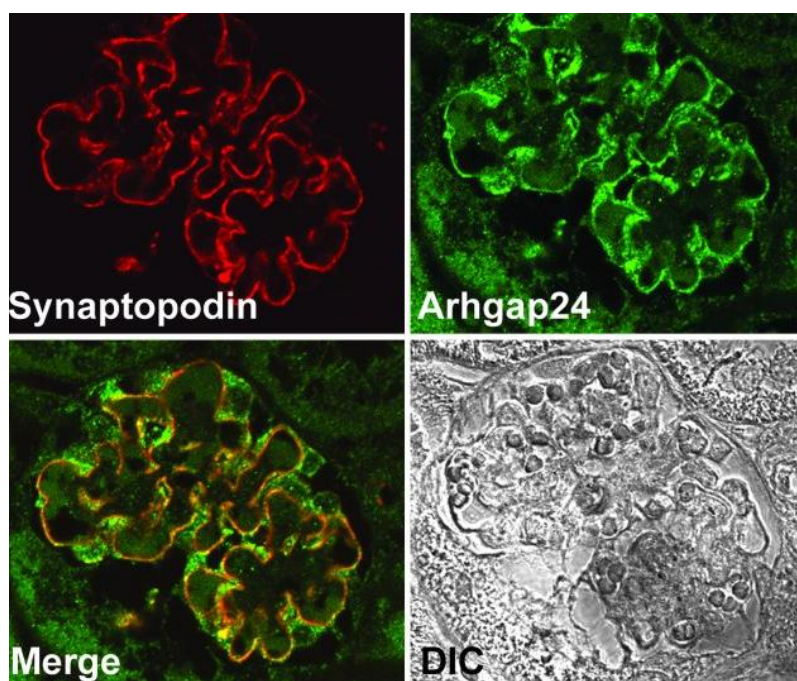
When undifferentiated podocytes were cultured at the permissive temperature, they exhibited highly ruffled plasma membranes. In contrast, the plasma membranes of the differentiated podocytes had a very smooth, flat appearance.

Cells were outfitted with a temperature-sensitive SV40 large T antigen. Heat them up and off they go.

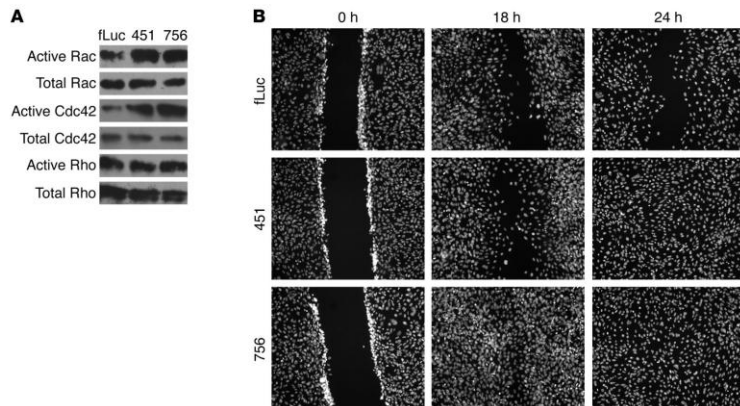
Podocytes upregulate Arhgap24 when they differentiate.



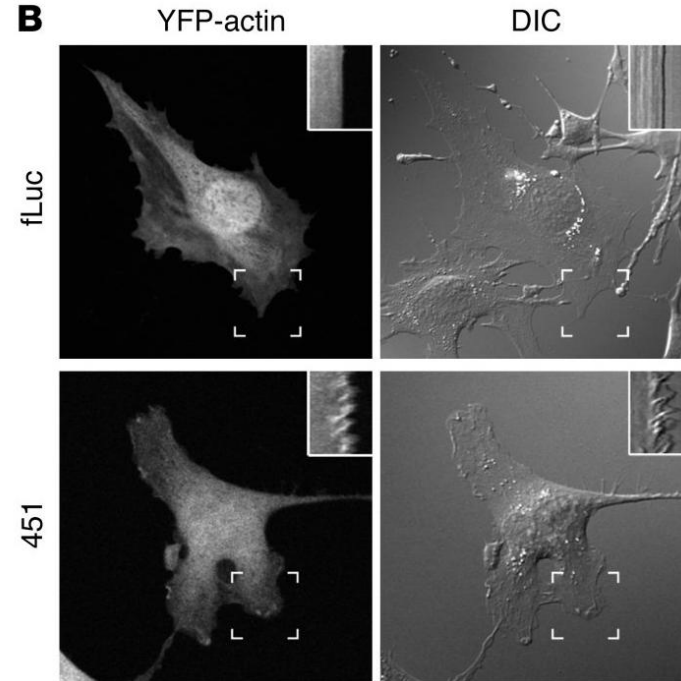
Arhgap24 colocalizes with the focal adhesion marker vinculin at the tips of actin stress fibers.



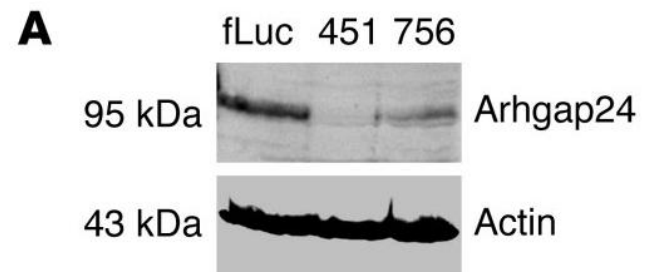
Arhgap24 is expressed in kidney podocytes in vivo.



Arhgap24 knockdown in differentiated podocytes increases active Rac1 and Cdc42 levels and accelerates epithelial monolayer wound closure. (Cells migrate and close the gap)



Arhgap24 knockdown in differentiated podocytes increases membrane ruffling.



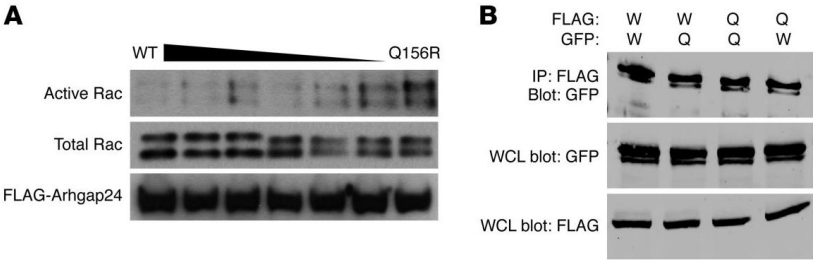
Recall that CDC42 was also up in INF2 mut

Incidence of *ARHGAP24* nonsynonymous sequence variations in patients with biopsy-proven FSGS (*n* = 310) and controls (*n* = 180)

Variation	No. affected	No. controls
Isoform 1		
T97I	1	0
R142C	1	0
Q158R	2	0
L215V	0	1
Q359R	0	1
S396L	1	0
P417A	9	2
T451I	1	0
T481M	2	0
F539L	5	5
N587I	0	1
Isoform 2		
P2L	3	1
R5L	1	0

Sequence alignment of the Arhgap24 protein across various species in the region of the patient variation (Q158R) showing the glutamine residue

Species	aa	Sequence	aa
<i>Homo sapiens</i>	141	vryekrygnr lapmlve Q cv dfirqrglke	170
<i>Pan troglodytes</i>	330	vryekrygnr lapmlve Q cv dfirqrglke	359
<i>Mus musculus</i>	139	vryekrygnr lapmlve Q cv dfirqrglke	168
<i>Rattus norvegicus</i>	140	vryekrygnr lapmlve Q cv dfirqrglke	169
<i>Callithrix jacchus</i>	141	vryekrygnr lapmlve Q cv dfirqrglke	170
<i>Equus caballus</i>	140	vryekrygnr lapmlve Q cv dfirqrglke	169
<i>Bos taurus</i>	46	vryekrygnr lapmlve Q cv dfirqrglke	75
<i>Canis familiaris</i>	58	vryekrygnr lapmlve Q cv dfirqrglke	87
<i>Gallus gallus</i>	141	vryekrygnr lapmlve Q cv dfirqrglke	170
<i>Monodelphis domestica</i>	156	vsfekrync lapmlve Q cv dfirqwgllke	185
<i>Danio rerio</i>	144	vryerygnk mapmlve Q cv dfirnwgllre	173



Arhgap24 Q158R has defective Rac1-GAP activity and dimerizes with the wild-type protein.

This genetic syndrome was solved by

1. Linkage analysis
2. Genetic association
3. Positional cloning strategy
4. Haplotype analysis
5. Basic research